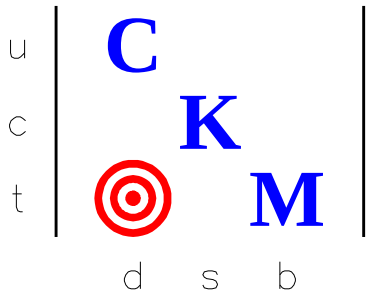

Charged Kaons at the Main Injector

June 4, 2001

Answers to PAC & Technical Review Committee Questions

J. Frank, S. Kettell, R. Strand
Brookhaven National Laboratory, Upton, NY, USA

L. Bellantoni, R. Coleman, P.S. Cooper*, T. R. Kobilarcik, A. Kushnirenko, C. Milstene, H. Nguyen, E. Ramberg, R. S. Tschirhart, H. B. White, J. Y. Wu
Fermi National Accelerator Laboratory, Batavia, IL, USA

G. Britvich, A. V. Inyakin, V. Kurshetsov, L. G. Landsberg,V. Molchanov, V. Obraztsov, S. I. Petrenko, V. Polyakov, V. I. Rykalin, A. Soldatov, M. M. Shapkin, O. G. Tchikilev, D. Vavilov, O. Yushchenko
Institute of High Energy Physics, Serpukhov, Russia

V. Bolotov, S. Laptev, A. Polarush, A. Pastsiak, R. Sirodeev
Institute of Nuclear Research, Troisk, Russia

J. Engelfried, A. Morelos
Instituto de Fisica, Universidad Autonoma de San Luis Potosi, Mexico

M. Campbell, R. Gustafson, M. Longo, H. Park
University of Michigan, Ann Arbor, Michigan 48109

R.K. Clark, C.M. Jenkins
University of South Alabama, Mobile, Alabama 36688

K. Lang
University of Texas at Austin, Austin, Texas 78712

C. Dukes, R. Godang, L. Lu, K. Nelson
University of Virgina, Charlottesville, VA 22901

* Spokesman: P.S. Cooper, pcooper@fnal.gov, (630) 840-2629

Web Address: www.fnal.gov/projects/ckm/Welcome.html

Contents

List of Figures

List of Tables

1 Written Questions from The PAC

1.1 Degradation due to missed performance specifications.

Q1. *Analyze the degradation of the signal if any of the elements of the detector or beam do not meet their performance specifications, including resolutions, efficiencies, stability, mechanical tolerances and defects in beam structure.*

Given the broad nature of the question, we must first appeal to the considerable amount of material in the written proposal which address these issues. However, we will attempt here to summarize some of the most important aspects of this question.

To begin with, the signal can be considered to be degraded in one of two ways: either there is a significant loss in signal yield for some reason, or the signal becomes dominated by background. Of course these are related in the sense that if you have to make more stringent background cuts then you lose acceptance. But we can consider these as separate issues for the sake of clarity.

The signal yield (for a given branching ratio) depends on the flux of incoming K^+ particles, the geometric acceptance and the kinematic acceptance. We have made many studies of the beam line and have concluded that the kaon rate is not significantly effected by typical tolerances found in other beam lines at Fermilab (see Tables 12 and 13 on pages 78 and 79 of the CKM proposal) and can be compensated for by small changes in various beam line elements (such as the beam stopper size). The geometric acceptance for kaon decays is most likely accurately determined by our GEANT Monte Carlo. In fact, the apertures of the elements in our spectrometer do not have a significant affect once we have made our kinematic cuts on the π^+ momentum and decay angle. Thus it is our knowledge of the resolutions and efficiencies of our sub-detectors that drives our knowledge of signal acceptance. We have accordingly placed great emphasis throughout our proposal on a detailed understanding of the resolution of each sub-detector. We have found a good correspondence between analytical calculations, GEANT simulations and data from similar existing detectors under operating conditions. Of course the yield will scale directly with the efficiency but it is typical to achieve above 95% efficiency in tracking detectors and phototube RICH detectors. Stability of each sub-detector is important, but more important is our ability to measure positions in situ. Given the flux of halo muons and nearly mono-energetic beam, we feel that there will be sufficient information on short time scales to track instabilities.

Of far greater concern than decreased signal yield due to resolution, efficiency or stability effects is how the background depends on these parameters. From several simulations of our detector, we have come to the conclusion that the main sources of background to our signal will be from $K \to \pi^+\pi^\circ$ decays, hadronic beam interactions in the last KEAT station and perhaps accidental effects where there are two nearly simultaneous K^+ decays. We take these individually:

- $K \to \pi^+\pi^\circ$ (Kpi2): The rejection against the Kpi2 background comes primarily from vetoing the photons accompanying π° decay, and then from kinematic rejection. We have made many studies of photon veto efficiencies and it is clear from those studies that our global π° vetoing inefficiency is nearly linearly dependent on the efficiency of vetoing very high energy photons (> 1 GeV) and to a lesser extent on the efficiency of vetoing very low energy photons (< 20 MeV). We have found that we can observe the required high energy vetoing inefficiency in already existing detectors, using electrons (see section 5.6.13). Our studies indicate that the physics limitation to high energy vetoing is about an order of magnitude less than our requirement. On the kinematic rejection front we have found in simulations that practically all of the Kpi2 background comes from real scatters in the material immediately up and

downstream of the vacuum decay region, not from resolution effects. We have made a simple study, using our latest high statistics Kpi2 simulation, of what the effect of increasing our missing mass resolution is. The result is that if the true missing mass resolution is 10% higher than we expect, then the effective branching ratio from Kpi2 goes from (6.7 ± 1.0) to (9.7 ± 1.3) $\times 10^{-12}$. If the resolution is 20% higher than we expect, then the Kpi2 background level is about (15 ± 2.0) $\times 10^{-12}$. Our nominal missing mass resolution can be improved by increasing our analyzing magnetic field strength and we are planning studies now to determine whether this extra safety factor is called for.

- Beam interactions: Our latest estimates for the level of beam interaction background is that it is less of a problem than Kpi2 decays. We have plans to continue our studies of this issue in greater detail. The level of this background clearly scales linearly with how much material there is in the beam line at the upstream end of the vacuum decay region. Great attention will be paid to the construction of the detector at this point. The main vetoing power against these upstream interactions is the BIVS system. We have shown with extensive simulations that the vetoing inefficiency of this device is not significantly dependent on its energy threshold (Figure 152 on page 216 of the CKM proposal). We will revisit the issue of kinematic rejection of hadronic scattering events with a high statistics GEANT simulation, but resolution effects will probably not dominate the rejection.

- Accidental effects: The background arising from two kaons decaying nearly at the same time has been estimated to be at the level 0.5×10^{-12}. Spatial resolution may not be as important a tool as temporal resolution on reducing the level of this background. Changes in the beam structure will have the biggest effect on this background, since it will more often drive two kaons closer together in time. The accidental background will scale as the square of the (instantaneous/average) beam intensity. Our accidental background estimates have assumed a 10% envelope on the (instantaneous/average) ratio. If this radio grows as large as ≈ 2, then our accidental background estimates will increase by about $\times \approx 4$, which are still below our Kpi2 background estimates.

1.2 Branching ratio systematic uncertainties

Q2. *Provide an estimate of the systematic uncertainties that may be obtained in the experimental quantities that enter into the branching ratio.*

In calculating a branching ratio, the relevant quantities are flux, signal acceptance and background. We address the systematic uncertainties in each of these.

1 Flux: Counting the incoming beam will be determined experimentally quite well. We rely on the fact that each beam particle will be observable. We estimate the global reconstruction efficiency of the UMS system as 99%, based on actual reconstruction efficiencies obtained from the HyperCP experiment (p.104). Tagging the species of incoming particles is done by the kaon RICH, where the pion and kaon ring radii differ by about a factor of 2 (p.117). There is only about a 1% chance of spatial overlap of beam particles in the UMS system and a 3% chance of temporal overlap in the kaon RICH system, so pileup effects will be able to be resolved cleanly. A reasonable estimate on systematic error for flux is 1%.

2 Acceptance: The geometric and kinematic acceptance for our signal will be determined primarily from a Monte Carlo simulation. This is typical of rare decay experiments. An example

of a similar experiment would be KTeV, which consistently quotes systematic errors on acceptance in the 1-3% range. The decay modes $K_{\mu 2}$ and $K_{\pi 2}$ would be excellent calibration decays for which we can compare Monte Carlo predictions with data. Both have a single secondary charged particle and can be identified cleanly in our experiment. Probably the dominant systematic uncertainty in the acceptance will be related to how we identify π^+ as they hadronically shower in the FVS/MVS system. Again, triggering on an unbiased $K_{\pi 2}$ sample should map out all the details of how this system responds to π^+ in our momentum range.

3 Background: We expect on the order of 10 background events for a 95 event signal in our experiment (see chapter 7 and Appendix of proposal). We have identified ways in which we can systematically increase our level of background and measure this increase (chapter 8). The statistical uncertainty for knowing the background level is interpolated from large samples outside the signal region. This uncertainty is negligible. We believe that we can conservatively hold the systematic uncertainty in the interpolation to 50% of the background subtraction.

The effects identified here would result in less than a 6% systematic uncertainty in the elements that make up the branching ratio. When added in quadrature with the 10% statistical uncertainty expected from a sample of 105 events with 10 ± 5 background events the total branching ratio uncertainty is 12%

1.3 Event rate and event size going to mass storage

Q3. *What is the event rate and event size going to mass storage and what are the implications for feasibility?*

A first estimate of the CKM events size is 5Kb for all data in a 200 nsec time window around the time of a level 1 (L1) trigger. L1 vetos $K \to \mu^+\nu$ decay and suppresses $K \to \pi^+\pi^\circ(K_{\pi 2})$ decays by about a factor of 10. Combining the 220 KHz L1 trigger rate with 200 KHz for prescales, calibrations and other triggers the data rate into the level 3 (L3) online processor farm is 2.1 Gb/beam-sec. The total clock time for the experiment is $3.3 \times 10^7 sec$ collected over 2 full years (2×39 weeks/year) of data taking. The spill structure is 1 beam-sec every 3 clock-seconds.

At L3 with full software we should be easily able to reduce $K_{\pi 2}$ decays significantly by rejecting candidates with energy deposits in either the VVS or FVS well above 1 MIP and away from the charged track in the FVS. What will remain is a set of pre-scaled background triggers and histograms from rejected triggers. The actual sample of signal candidates at this level is negligible. A net rejection factor at L3 of 20 would lead to a 1155 Tb data set sent to long term storage as 7 KHz of 5 Kb events. This is $\times 6$ the volume of the total KTeV raw data set (200 Tb). For comparison the L3 rejection factors for Selex and KTeV were each about 10 with Selex data dominated by background and KTeV data dominated by signal.

Based upon experience from Selex, KTeV and other experiments with Level 3 filter farms the level of computing required for such a level 3 algorithm is 100 instructions/byte (I/b). Our level 3 would require about $4.3 Gb/sec \times 100 I/b = 430 GI/sec$, or about 400 present day Linux-PC's with 1.1 GI/sec processors. Such a system would cost about \$500K today. This plan seems feasible with even today's standards for offline storage and computing. We are told that we are in no danger of running for at least 5 years. Moore's law scaling would be about a factor of $\times 10$ in price performance over that period.

CKM Data Rates and Volumes

Level	Input Rate	Data size	Input Volume	Rejection
1	continuous	all hits	13 Gb/beam-sec 4.3 Gb/sec	15
3	4.2×10^5/beam-sec 140 KHz	5 Kb	2.1 Gb/beam-sec 700 Mb/sec	20
storage	7 KHz	5 Kb	35 Mb/sec	1
total	2 years=$3.3 \times 10^7 sec$		1155 Tb	

Table 1: CKM proposal data rates and volumes.

For comparison we have included in table 2 below the same rates from the BTeV proposal (figure 9.1, page 118) as shown for CKM in table 1 above. Some interesting conclusions emerge from this comparison. The total data volume buffered at the front ends of BTeV is two orders of magnitude higher that CKM. They, of necessity, apply significant rejections in each of their 3 levels of trigger. CKM has a L1 rejection of 10 against $K_{\pi 2}$ and a large L1 rejection against $K_{\mu 2}$. We have no rejection at L2. In fact we have no real L2, only a place holder.

BTeV is a Collider experiment. For them, a beam-second is a clock-second. CKM gets 2/3 seconds to move data around and to compute when there is no beam. The time averaged data rate that BTeV has entering their Level 3 farm equals the time averaged total data volume going into the CKM front-ends. This implies that if CKM chose to adopt a similar network and data switching strategy to BTeV we could do the Level 1 trigger in software in the Level 3 farm. This is a technical choice, to be made latter, driven by relative cost and convenience considerations. It does illustrate the relative challenges in high volume data transfer and required trigger rejection faced by the two experiments.

BTeV Data Rates and Volumes

Level	Input Rate	Data size	Input Volume	Rejection
1	7.6 MHz	200 Kb	1500 Gb/sec	100
2	100 KHz	200 Kb	20 Gb/sec	5-10
3	20 KHz	200 Kb	4 Gb/sec	5-10
storage	4 KHz	40 Kb	160 Mb/sec	(compression) 5
total	2 years=$3.3 \times 10^7 sec$		5300 Tb	

Table 2: BTeV proposal data rates and volumes.

BTeV's total data volume to storage; running for the same 2 years as CKM, would be 5300 Tb. This assumes a data compression of a factor of 5 from 200 Kb/event to 40Kb/event. This data volume is $\times 4.6$ times our estimate for CKM.

Again calling on experience from previous experiments: the offline computing required for event reconstruction is $> 10,000$ I/b for a Collider type experiment (CDF and Dzero run 1 reconstruction codes were in this region). The KTeV analysis code required 200-500 I/b of CPU for reconstruction, due to their simpler events. In CKM an ideal event has exactly one charged track in each charged

particle detector and no vetos fired in time. The number of large combinatoric problems, which tend to dominate CPU requirements, are quite limited for CKM data, as they were for KTeV data. The combination of the smaller volume of data stored and the much lower CPU requirements per byte of data will make the CKM offline computing needs a few percent of BTeV's requirements.

1.4 Veto system intermittent failures

Q4. *Explain how intermittent failures in the veto system will be monitored to the required level.*

Our analysis of $K \to \pi^+\pi^0$ background in the proposal concludes that the asymptotic inefficiency requirements at high energy for the VVS (Vacuum Veto System) and FVS (Forward Veto System) are 3×10^{-5} and 1×10^{-4} respectively. We have argued that physical mechanisms of inefficiency at high energy (e.g. photo-production) are far below these requirements, and that readout system failures are the greatest concern. Clearly the rate of coherent intermittent system failures of the VVS and FVS must be kept below the respective asymptotic single photon inefficiency specs. At the other end of the failure scenario spectrum, a *single* channel in the VVS or FVS (~ 2000 channels each) can be dead for no more than 6% and 20% respectively per event. The failure mechanisms that we will encounter in the field will more likely exist between these two extreme scenarios.

In section 5.6.14 of the proposal we discuss a multi-tiered monitoring system that has the following elements:

- Each VVS and FVS photo-multiplier tube will be flashed with a LED or laser fiber at a rate of 1 Hz. This will ensure that each channel is live before, during, and after the one second spill that arrives every three seconds.

- Each VVS photo-multiplier instruments a sector of lead-scintillator stack that is physically interleaved with a neighboring readout channel. This allows high energy deposits in the VVS to be cross-monitored by at least two photo-multiplier channels. Essentially all of the data readout during the spill will be calibration sets, which will include $K \to \pi^+\pi^0$ decays that are identified only with spectrometer information. These minimum bias data sets will be used to cross monitor high energy deposits in the VVS.

- The large fluence (7 MHz) of traversing high energy muons can be exploited to continuously monitor the the VVS and FVS throughout the spill. High energy muons can be directly tracked by the spectrometer to the FVS, and the geometry of the VVS can be used to coarsely track muons that traverse the VVS outside the acceptance of the spectrometer.

- As argued in section 5.6.14, minimum bias $K^+ \to \pi^+\pi^0$ decays can be used to directly measure the global π^0 inefficiency of both the VVS and FVS. Enough minimum bias data can be taken every few days to measure the global π^0 inefficiency without over-taxing the data acquisition or analysis facility. If a global efficiency problem is found, high energy photons from $K \to \pi^+\pi^0$ can be pointed with sufficient accuracy to isolate under-performing regions of the veto system.

These monitoring tools will allow CKM to monitor single photon (channel) efficiencies to the required level. It is important to realize however that the requirement on coherent system failure in the VVS is far more stringent than the single photon efficiency, since both photons from $K \to \pi^+\pi^0$ most often intercept the VVS. Achieving the required π^0 inefficiency of 1.6×10^{-7} implies that the

rate of coherent system failure in the VVS must be held to less than the 1.6×10^{-7} level per event. Coherent failures can come in a variety of insidious forms at this level, ranging from global HV glitches to data banks within an event being scrambled. Our strongest weapon in controlling coherent failures in this regime is the structure of the CKM event discussed in proposal section 6.2. Each CKM event will record several hundred nanoseconds of fully live time prior to the event trigger time. Given the fluence of muons (7 MHz) and high rate of K^+ decays (6 MHz), each CKM event will have a one or more "calibration" muons or K^+ decays that will ensure that the veto system is locally live in time and data structures.

While we are confident these strategies will enable CKM to monitor efficiencies at the required level, it is useful to study what has already been achieved with similar detector systems. In the proposal we have presented efficiency studies from KTeV data of high energy electrons from $K_L \to \pi^{\pm} e^{\mp} \nu$ that illuminate both lead-scintillator and CsI detectors. These studies demonstrate that detection inefficiencies of less that 3×10^{-5} can be achieved with real detectors operating under real battle conditions. Further, BNL experiment E787 has demonstrated a π^0 inefficiency of 6×10^{-7}, and hence global system inefficiencies are controlled to at least that level. CKM is required to push this achieved level of system efficiency control by a factor of $\times 4$ to a π^0 inefficiency of 1.6×10^{-7}.

1.5 Missing mass spectrum in relevant categories

Q5. *Provide the missing mass spectrum of the background divided into relevant categories such as event topologies.*

From our various simulations of CKM we have determined that the dominant source of background to the $K^+ \to \pi^+ \nu \bar{\nu}$ signal is from mis-measurements of $K^+ \to \pi^+ \pi^0$, or Kpi2, decays. We discuss here the characterization of Kpi2 background events in our latest simulation.

In our recent studies with the GEANT based CKM Monte Carlo we had 52 events out of 10 Million generated Kpi2 decays which passed all the cuts. These cuts are strictly kinematic, with the final cut being on missing mass. This level of background corresponds to an effective branching ratio of 6.7×10^{-12}, or 6.7% of the expected $K^+ \to \pi^+ \nu \bar{\nu}$ signal size.

The mis-measurement of missing mass in these events is too big to come from resolution tails. So the above 52 events were reproduced in our GEANT Monte Carlo and studied with the assumption that either the kaon or the pion track had been deflected after (for K) or before (for π^+) it was measured. We printed out each step where GEANT deflected a track at an angle above a threshold of .75 mRad.

Indeed, 48 of the 52 events had such a large scattering step. We are currently studying the other 4 events to determine their background mechanism. The detailed results are presented in Table 3. Here is a brief summary:

- In half of the cases the deflected track was the kaon and in the other half it was the pion.
- In all cases but one the scattering occurred near the last KEAT station or the first DMS station. The exception had a large scatter in the pion RICH.
- In most cases (37 out of 48) the reason for the deflection was identified by GEANT to be a Coulomb scattering as generated by Moliere theory. In 11 cases a hadron elastic scattering was the cause for the contribution to the background.
- Of 24 kaon tracks
  - 12 scattered in material of the downstream KEAT station.
  - 8 scattered in the vacuum decay volume entrance window
  - 4 scattered in either the helium bag or air gap between the KEAT stations or in the air gap between the downstream KEAT station and the vacuum window
- Of 24 pion tracks
  - 23 scattered in the material of the first straw tube station
  - 1 scattered in the Pion RICH gas

Of course such a scattering event should not have passed our analysis cut on DOCA (distance of closest approach between the kaon and pion tracks) unless the scattering plane is close to the same as the decay plane. To check this we histogrammed the angle between these two planes (see Figure 1, where the scale is in degrees). This data shows that the scatter plane and decay plane are definitely correlated.

We conclude from our studies that the background to our signal coming from Kpi2 decays, as determined by GEANT, is due primarily to elastic Coulomb scattering in the material nearest the vacuum decay volume.

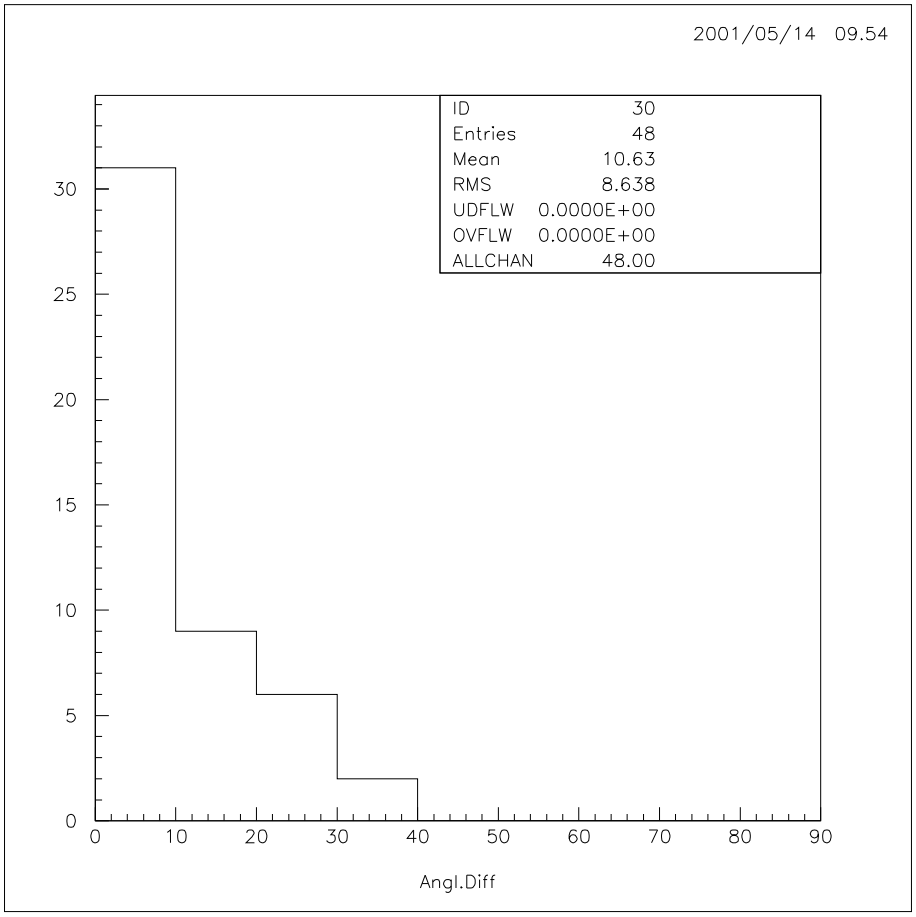

Figure 1: The angle between decay and scatt. planes

Table 3: $K\pi 2$ background studies results

Part	Volu	Z	Step	Sang	Sn	AngD	PhD	phS	Ev	Mechanism
K+PI2	CATH	13450	0.0025	3.76	0.084444	4.844222	0.954794	1.039338	028	NEXT LOSS MULS
K+PI2	CATH	1344.00	0.0025	1.41	0.415551	24.554720	2.719554	2.291007	010	SCOR NEXT LOSS MULS
K+PI2	CATH	1344.50	0.0025	1.17	0.001656	0.094863	-1.657458	-1.655807	051	NEXT LOSS MULS
K+PI2	CATH	1344.50	0.0025	1.85	0.110827	6.363156	0.601519	0.712573	029	NEXT LOSS MULS
K+PI2	CATH	1345.00	0.0025	1.37	0.015159	0.868580	-1.459319	-1.444160	003	NEXT LOSS MULS
K+PI2	KTV1	1346.00	0.00103.79		0.078649	4.511028	-2.960706	-3.039436	035	LOSS MULS HADR ECOH
K+PI2	KTX1	1344.50	0.4974	2.29	0.003860	0.221150	-2.629396	-2.625536	011	NEXT LOSS MULS
K+PI2	KTXX	13475	0.0010	1.99	0.377770	22.196282	2.405955	2.793341	037	LOSS MULS HADR ECOH
K+PI2	POLY	13400	0.0025	1.25	0.212091	12.245268	1.465618	1.679332	045	NEXT LOSS MULS
K+PI2	POLY	13400	0.0025	1.85	0.106738	6.127475	-0.351326	-0.458267	002	NEXT LOSS MULS
K+PI2	POLY	1347.00	0.0026	1.51	0.089324	5.124888	1.420928	1.331484	050	SCOR NEXT LOSS MULS
K+PI2	POLY	1347.00	0.0028	.35	0.070485	4.041982	-1.449112	-1.378569	031	NEXT LOSS MULS
K+PI2	VVWN	1358.49	0.0108	1.61	0.049413	2.832403	-0.227156	-0.276589	016	LOSS MULS HADR ECOH
K+PI2	VVWN	1358.51	0.0255	2.37	0.033967	1.946607	-2.617595	-2.651569	018	LOSS MULS HADR ECOH
K+PI2	VVWN	1358.52	0.03513.68		0.380099	22.340486.080731		-2.812552	041	LOSS MULS HADR ECOH
K+PI2	VVWN	1358.52	0.0381	1.26	0.017996	1.031192	-0.844891	-0.826894	021	NEXT LOSS MULS
K+PI2	VVWN	1358.52	0.0381	1.61	0.264389	15.331093	2.299140	2.566710	046	NEXT LOSS MULS
K+PI2	VVWN	1358.52	0.0381	1.81	0.172316	9.922813	-1.040355	-0.867174	006	NEXT LOSS MULS
K+PI2	VVWN	1358.52	0.0381	2.04	0.111402	6.396342	2.060267	2.171900	020	NEXT LOSS MULS
K+PI2	VVWN	1358.52	0.0381	2.64	0.069208.968604		-1.094641	-1.025378	017	NEXT LOSS MULS
K+PI2	CKM	13400	5.0000	2.11	0.158920	9.144502	1.883620	2.043217	019	NEXT LOSS MULS
PI2	CKM	1357.65	10.6527	2.55	0.056438.235452		1.926168	1.982635	049	LOSS MULS HADR ECOH
CKM		1358.48	11.4809	1.71	0.611534	37.701636	-0.784697	-1.442694	005	NEXT LOSS MULS
HEKT		1338.00	306.0001	1.35	0.000268	0.015347	1.571974	1.571707	014	NEXT LOSS MULS
PRGA		6968.90	1209.2778	1.69	0.248884	14.4118823.039643		-2.992034	042	CKOV LOSS MULS DRAY
TGA		4660.96	0.1942	1.61	0.010605	0.607644	0.280066	0.269462	009	LOSS MULS HADR ECOH
TKP		4658.88	0.00203.36		0.293806	17.086470	1.184256	0.886051	027	LOSS MULS HADR ECOH
KP		4659.24	0.0043	1.12	0.113208	6.500442	2.031443	2.144887	007	NEXT LOSS MULS
KP		4659.25	0.0033	2.66	0.265207	15.379716	-0.496893	-0.228476	033	NEXT LOSS MULS
KP		4659.46	0.0198	1.91	0.471447	28.129076	2.406312	1.915404	048	NEXT LOSS MULS
KP		4659.55	0.0178	1.00	0.041423	2.374134	0.959808	0.918377	052	NEXT LOSS MULS
KP		4659.71	0.0041	1.41	0.197268	11.377605	1.257358	1.455916	004	NEXT LOSS MULS
KP		4659.74	0.0032	2.42	0.167933	9.667967	2.529537	2.698267	008	NEXT LOSS MULS
KP		4659.75	0.0020	1.75	0.534495	32.310627	-2.798638	-2.234769	039	LOSS MULS HADR ECOH
KP		4659.82	0.0046	1.27	0.419680	24.815133	-2.960002	-2.526944	001	NEXT LOSS MULS
KP		4659.84	0.0049	1.48	0.282969	16.437950	-0.618251	-0.331375	026	NEXT LOSS MULS
KP		4660.16	0.00513.03		0.113279	6.504540	-1.538689	-1.425169	012	NEXT LOSS MULS
P		4660.18	0.0048	1.76	0.478069	28.560199	2.870503	2.372080	040	NEXT LOSS MULS
P		4660.29	0.0000	2.08	0.096582	5.542536	-2.522980	-2.426250	034	LOSS MULS HADR ECOH
P		4660.33	0.0044	1.51	0.156333	8.994351	-2.725851	-2.568887	047	NEXT LOSS MULS
P		4660.41	0.0083	1.02	0.259240	15.025391	1.150684	0.888463	032	NEXT LOSS MULS
P		4660.69	0.0045	2.69	0.118691	6.816769	1.681920	1.800890	043	NEXT LOSS MULS
P		4660.69	0.0047	1.09	0.076933	4.412421	2.332027	2.409031	022	NEXT LOSS MULS
P		4660.72	0.0040	1.41	0.073281	4.202558	1.935389	1.862046	013	NEXT LOSS MULS
P		4660.77	0.0034	1.69	0.087041	4.993532	-2.341186	-2.254039	024	NEXT LOSS MULS
P		4661.11	0.0061	2.32	0.127566	7.329165	-0.166128	-0.038216	036	LOSS MULS HADR ECOH
P		4661.14	0.0072	1.46	0.261371	15.151873	-3.011874006886		023	NEXT LOSS MULS
661.02			0.0020	0.75	0.157106	9.039206	-1.306638	-1.148892	038	NEXT LOSS MULS

Table 3: (continuation) table fields description

```
  Column description
  ====================
  Part - particle
  Volu - GEANT volume name (see below)
  Z    - z coordinate at the end of the step
  Step - step length
  Sang - scattering angle (mrad)
  Sn   - sin of the angle between the decay and the scattering planes
  AngD - angle between the decay and the scattering planes (in degrees)
  PhD  - phi of the vector perpendicular to decay plane
  phS  - phi of the vector perpendicular to scatt. plane
  Ev   - event number
  Mechanism - GEANT mechanisms involved in the given step
              (ECOH stands for Elastic COherent Hadronic scattering, MULS - multiple scattering)


  Volume description (See also Fig.1)
  ===================================

  POLY, CATH, KTXX - Windo, cathode plane and gas volume of the downstream KEAT (Kaon Entrance Angle Tracker)
VVWN             - Vacuum Window at the entrance to the decay volume
HEKT, CKM        - Helium bag between KEAT Stations, air in gaps between the helium bag, the downstream KEAT and
                   the vacuum window

STKP             - walls of the upstream straw tube station
STGA             - gas in the upstream straw tube station
STSW             - wires of the upstream straw tube station
PRGA             - gas in the Pion RICH
```

Figure 2 is a plot of the missing mass squared as reconstructed by the RICH vs. the missing mass squared as reconstructed by tracking (from the magnetic spectrometer) for 10 million event $K^+ \to \pi^+\pi^0$ GEANT Monte Carlo run (including the 52 background events). This Figure is similar to Figure 148 on page 212 in the CKM proposal, except that it has none of the cuts that correlate the missing mass measurements. Consequently, this Figure shows no apparent correlations. This is consistent with the independent measurement processes of the momentum from the tracking (from the magnetic spectrometer) and the velocity vector measurement (from the RICHs).

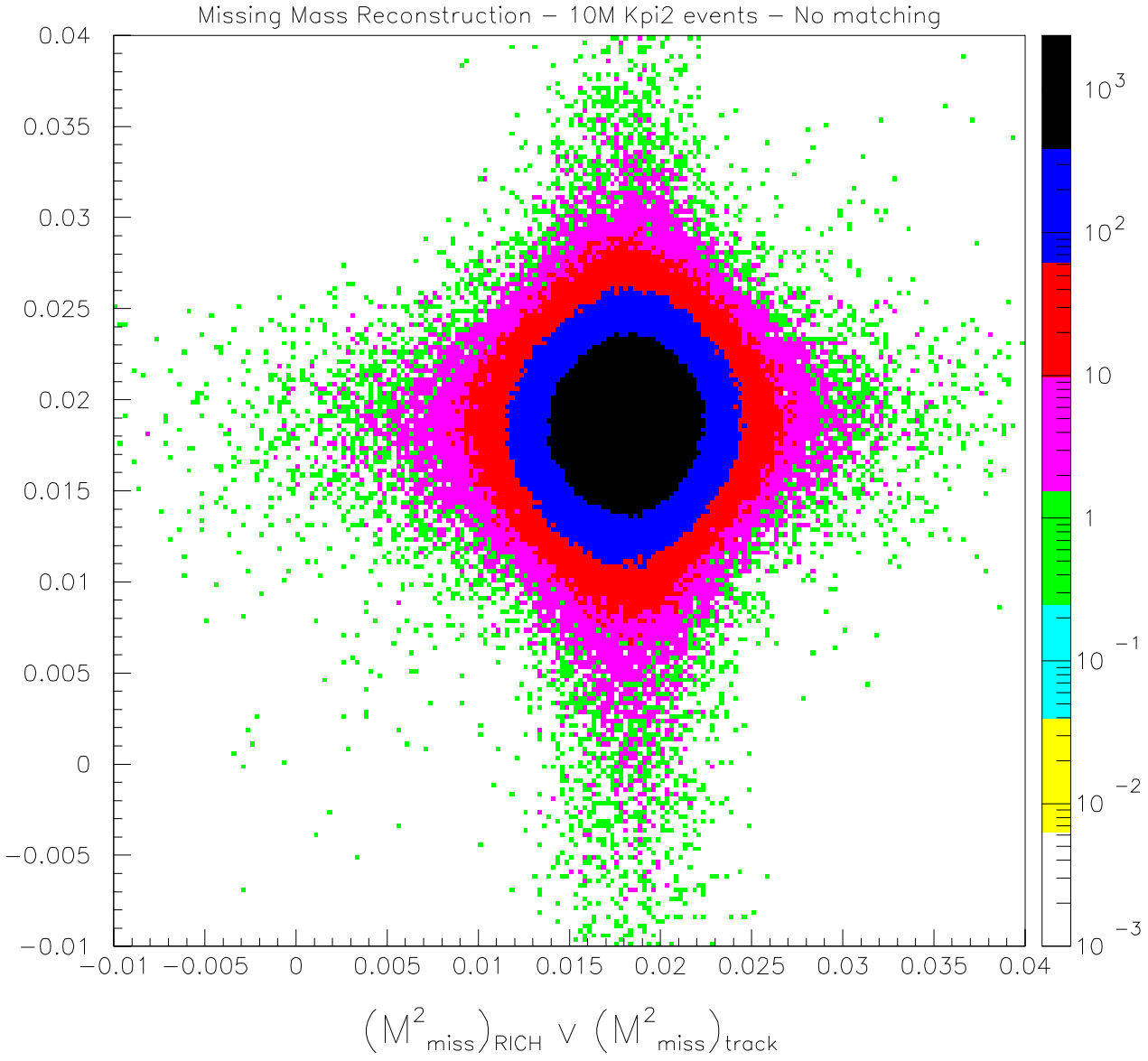

Figure 2: The Missing mass squared as calculated by the RICH system vs. tracking.

1.6 Optimal timeline for commissioning the RF separated beam

Q6. *What timeline is optimal for commissioning the RF separated beam and testing the kaon purity?*

The *optimal* timeline for commissioning and testing the RF separated beam, like the optimal timeline for verifying that the detector achieves the necessary level of background rejection, envisions a conventional (non-superconducting) beam line's existence relatively early in the project's life. Proceeding promptly on the civil construction and on forming the beam line means these structures can function like a "backplane" into which both the RF separator and the detector elements needed for the factorization test can be inserted.

We plan to test superconducting cryomodules with full RF power in a beam with facilities that exist or will be purchased soon after approval. Those tests will tell us about the basic functionality of the system, it's stability over long time periods, its susceptibility to mechanical problems such as microphonics, its higher order mode excitations, and will give us a measurement of the amount of deflection per unit of RF power. The results of these tests should tell us how the modules will function in the designed beam line; but since these tests will be done in a beam that differs from the final beam in terms of intensity, energy and time structure, the following step will be to operate the cryomodules in the final beam line. Bearing in mind that R&D progress is notoriously hard to predict, we plan that these tests may be completed on first cryomodule by the end of 2003.

The creation and commissioning of the beam line should begin promptly after approval and proceed in parallel with the development of the cryomodules. The general activities are (1) the ME beam line infrastructure including the cryoplant, which appears to be a long lead-time activity; (2) new civil construction; and (3) installation and beam commissioning without superconducting elements. We must bring the primary beam to our target with the right spot size and good stability, and study its time structure. We also will need to measure muon rates and target-out rates, preliminary intensity tests to verify flux and production calculations, and we must check the beam instrumentation and controls. Previous experience and the recent review of the beam design also suggest a number of studies beyond the usual beam commissioning activities. These include an optics study to compare the actual beam to its design and Monte Carlo simulation, and scattering studies to determine the effects of tails of the beam.

A particularly significant milestone will follow the integration of two 5 MeV cryomodules in a well-understood beam line with refrigeration and RF power supplies. At that point we can produce a low rate (7 MHz) beam with a significantly enhanced kaon fraction. There is no particular relationship between this milestone and the background factorization test described in chapter 8 of the proposal; either may occur first. Following the first K^+ separation, cryomodules can be introduced in pairs until the final 15 MeV/station deflecting system exists.

1.7 Provide a list of FTEs

Q7. *Provide a list of FTEs, with names attached where they exist, of the collaborators and their commitments for construction.*

At the present time we have not assigned final responsibilities for construction the detector components. We thought it best to have a pie before we tried to carve it up. In the spirit of planning for success we have scheduled a week long group meeting at the end of July in Ann Arbor to begin this process in the experiment. With this caveat stated there are clearly strong interests and capabilities among the groups of the collaboration for most major components of the experiment.

It is highly likely that most or all of these will evolve into defined hardware responsibilities. These interests include:

- The design and ultimate construction of the CKM beam line will be a Fermilab responsibility lead by the Fermilab Beams Division members of CKM (R. Coleman, T. Kobilarcik, H. White)
- The deputy group leader of the SCRF effort in the Beams division is Leo Bellantoni who is a Fermilab Wilson Fellow. This project is in the R&D phase now and will become a construction project in due course.
- The University of Virginia group has considerable expertise and experience from HyperCP to take charge of and build the UMS / KEAT chambers. The Michigan group (M. Longo, D. Gustafston, H. Park) have also contributed to the design of the KEAT.
- THE UASLP group lead the design of both RICH system. They already have some Mexican funds for prototype mirrors and photo-multipliers. They will surely play an important role in leading the RICH effort in collaboration with groups much closer to the lab (e.g. the Fermilab group) who will have to worry about the large RICH components like the vessels and gas system.
- The design of the VVS and vacuum system have been lead by the Fermilab group (R. Tschirhart).
- The design and prototyping of the DMS straw-tube chambers has been lead by Hogan Nguyen who is a Fermilab Wilson Fellow. This project is in the prototyping phase now and will become a construction project in due course.
- The IHEP Protvino group has lead the design and prototyping of the muon veto system (MVS), including the test beam work done at Protvino.
- Design and leadership of the electronics efforts for CKM will come from a combination of people from Michigan (M. Campbell), Virginia (K. Nelson) and Fermilab (R. Tschirhart, J.Y. Wu)
- The simulation and analysis effort has been lead by Erik Ramberg of Fermilab with important contributions by members of the Fermilab, UASLP, IHEP and Virginia groups.

This list is not exhaustive. Not all present CKM groups are fully subscribed yet nor are all areas fully covered. We have need of, and room for, more collaborators both within the present groups and from new groups.

With four major national laboratories collaborating it is premature to list the technical staff available for detector construction of an un-approved proposal. The resources available are substantial at both the labs and the four university groups.

The commitments of the signatories of the CKM mast-head can be simply enumerated. The general principal is that CKM is the only new experimental commitment for the majority of the present collaborators. The caveats to this general principal are as follows:

- Four members of the Fermilab group (P. Cooper, A. Kushnirenko, E. Ramberg and R. Tschirhart) are also members of BNL E949. The agreement between Fermilab and BNL was that the contributions on the two experiments were to be comparable. The contributions of the BNL group to CKM (J. Frank, S. Kettell, and R. Strand) should offset the Fermilab group contribution to BNL E949.

- The IHEP Protvino group has a standing commitment to their laboratory to each spent half of their time working at home. This will mostly be on OKA, their new "medium rare" kaon decay program. The two IHEP group leaders (L. Landsberg and V. Obratsov) are on both CKM and KAMI. Two other members of the IHEP group are also on both experiments with the agreement that V. Molchanov will concentrate on CKM and V. Kurshetsov will concentrate on KAMI. Four members of the IHEP are also on BNL E949.
- Ken Nelson of Virginia is on both CKM and KAMI and will split his time between the two experiments.
- In the Michigan group Myron Campbell has present commitments to CDF and Atlas and Dick Gustafson has commitments to LIGO.

2 Verbal Questions from Technical Review Committee

The following questions were asked verbally by the technical review committee. We supply the questions and the answers for these verbal questions in this section.

2.1 Measurement of the π^0 detection inefficiency

Q1. *How will the π^0 detection inefficiency be measured in CKM?*

This question is addressed in Sections 5.6.14 and 8.2 of the proposal. That discussion is summarized here. We will employ a large sample of minimum bias $K^+ \to \pi^+\pi^0$ events that are collected with no requirements on photon veto response. We will then cut tightly on the RICH and magnetic spectrometers, and the muon veto system to define a very clean sample of $K^+ \to \pi^+\pi^0$ decays with a background of less than 1×10^{-7}. This low level of background in control $K^+ \to \pi^+\pi^0$ samples has been achieved by BNL-E787 in similar efficiency studies. This technique of course assumes that the tight selection criteria imposed on the incident K^+ and decay π^+ does not bias the photon veto efficiency. Demonstrating this factorization will require a detailed study, but the successful experience of BNL-E787 in generating similar samples suggest such low-background unbiased samples are attainable. This sample of $K^+ \to \pi^+\pi^0$ decays then is a $\pi^0 \to \gamma\gamma$ calibration sample where the π^0 decay vertex and momentum are well measured. Measuring the momentum of one "tag" $\pi^0 \to \gamma\gamma$ photon together with a π^0 mass constraint allows the momentum of the other "probe" photon to be determined. The precision of the inferred probe photon momentum is limited to the $100 - 200 MeV/c$ level by the precision with which the the parent K^+ momentum and decay $\pi^+$is measured. This is a liability of the in-flight technique that is not present in the stopped K^+ technique where the momentum of the parent K^+ is known with effectively perfect precision.

Although the energy and direction of low energy photons are not well measured, The integrated π^0 inefficiency of the detector can be measured with this sample. Further, the geometry of the CKM detector can be exploited to measure the single photon efficiency of the VVS separately where efficiencies are most critical. A π^0 that decays within the fiducial decay volume and deposits a well measured photon cluster in the FVS *must* have the other photon intercept the VVS somewhere. This assurance is a direct result of the large separation of the FVS from the upstream decay volume. These VVS probe photons can be used to measure the integrated VVS inefficiency from 0-200 MeV, with growing recovery of pointing accuracy and energy resolution with increasing inferred probe energy. Above 1 GeV, where VVS efficiencies are most crucial, the energy of the probe photon

within the VVS can be measured with a 10-20% precision, and with some reasonable pointing resolution. Similar pointing techniques can be used in the FVS where the energy of the probe photon is always above 1 GeV, which again is the result of the large distance of the FVS from the upstream decay volume.

Adequate $K^+ \to \pi^+\pi^0$ statistics can be collected every few days of running without over-taxing the data acquisition system. These quasi-realtime samples will allow the π^0 efficiency to to closely monitored throughout the two-year run.

2.2 Vacuum veto system filling fraction

Q2. *How much can the Vacuum Veto System filling fraction be increased from the nominal value of 50%?*

The lead-scintillator stacks that the VVS stations are mounted between two steel annular strong-back structures. The 50 cm long stations are separated by 50 cm gaps in our current design. This gap could be reduced to 15 cm and still allow for the simple strong-back suspension scheme. This would increase the active coverage fraction to 85% at the cost of significantly more lead, scintillator, and readout. Although the added safety factor would be welcome, the cost of high quality scintillator is a cost-driver for the experiment and such a design change would have to be carefully considered.

2.3 Conversion veto plane dead time

Q3. *What is the dead time due to the Conversion Veto Plane. Is there a hole in the Conversion Veto Plane, and if not, how do you handle the beam going through it?*

The beam rate at the CVP is about 40 MHz, the balance of the kaon component having already decayed. From Figure 25 on page 75 in the proposal the size of the beam there is about 50 mm wide. Assume that the CVP is identical in construction to the BTS. The average rate in the 1 mm fibers is $40MHz/50 = 0.8MHz$ with 1 nsec time resolution on each hit.

Take a $\pm 3\sigma = 6$ nsec wide veto gate around any trigger. 40 MHz $\cdot$ 6 nsec =24% of the time there will be another beam track close in time to a candidate. Our tracking finding efficiency for seeing this out of time beam track in the UMS is 98-99%. As we've said, we'll keep candidates with close in time beam tracks if we can follow those other tracks all the way through the system. The inefficiency due to an out of time beam track lost in the UMS but found in the CVP is $24\% \cdot (1-2)\% < 0.5\%$.

While we're at it let us anticipate your next question. "What about the loss from the 10MHz of kaons which decay before the CVP and therefore can't be tracked out of the system?" With the same assumptions as above this amounts to 10 MHz $\cdot$ 6 nsec = 6% of the candidates. 64% of these (4% of candidates) are Kmu2's which are already accounted for in the first entry of Table 37 on page 217. The remaining 2% are a salvage project - we could lose all of them as a worst case.

2.4 Correlations of the velocity and magnetic missing-mass measurements

Q4. *A potential mechanism for correlation of the velocity and magnetic missing-mass measurements is the variation of the field integral across the DMS spectrometer magnetic. The pion RICH measured momentum vector must be propagated back through the DMS magnet to recover the pion's decay angles. The RICH cannot measure position so only an average field*

integral is available without appealing to the straw-tube spectrometer for the track's position. Is this a problem?

We reproduce in Figure 3 the measured field integral as a function of transverse position across the face of the KTeV spectrometer magnet. This magnet is the model we have been using for the still undesigned CKM spectrometer magnet. The superimposed circle is the $40cm$ radius aperture of the VVS. The total variation in field integral across this aperture is $\pm 0.2\%$. The momentum resolution of the pion RICH is about 1%. The variation in field integral will make a negligible contribution to the overall pion RICH momentum resolution.

The data for Figure 3 were kindly provided by Doug Jensen of KTeV, KAMI, and Fermilab.

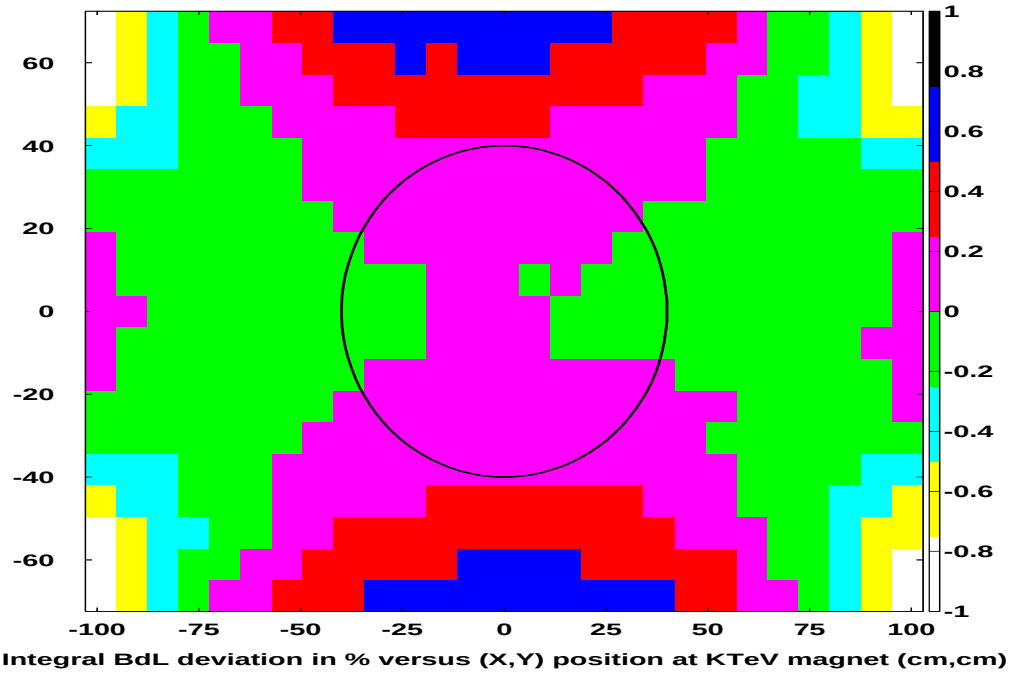

Figure 3: The fractional deviation [%] in the field integral of the KTeV spectrometer magnet across the face of the magnet aperture. The circle shows the aperture of the CKM VVS. The total deviation inside this circle is $\pm 0.2\%$

3 Written Questions from Technical Review Committee

Several questions were raised in the report of the technical review committee. We have abstracted what we understand to be the most important of these and supply the questions and the answers for these questions in this section.

3.1 DMS straw system technical feasibility

Q1. *The ability to make the DMS straw system operate successfully in a vacuum is a potential "show-stopper" for the experiment. What are the plans for demonstrating the the technical feasibility for this system?*

We concur with this concern and thus have dedicated a large fraction of the engineering made available to us, thus far, toward addressing it. We have already demonstrated acceptable mechanical strength ad leak rates of the straws in a vacuum. Our next goal is to build a prototype which can be operated, under vacuum, in a test beam. We note that the MECO experiment at BNL is undertaking a parallel development of a similar system.

Our general approach to the CKM apparatus is to adopt only well established techniques and to avoid serious detector development wherever possible. Operating straw-tubes in a vacuum and the development of 3.9 GHz SCRF cavities operating in transverse deflecting modes are the two major exceptions to this principal. As the committee notes, these are unavoidable since the experiment requires them in order to succeed. We've applied some of our best people to these problem as early as we could in order to remove these technical risks as soon as possible.

3.2 Fast and thermal neutrons in the VVS

Q2. *Are there data from KTeV which might inform us on the singles rates expected in the VVS from Fast and Thermal neutron?*

Yes, KTeV data does exist that can address this concern. Data from the E799 rare-decay run that was collected with a high energy 80 MHz neutral hadron beam can be used to estimate the dump neutron fluence induced by the 40 MHz CKM K^+ beam. The basic technique is to exploit the clocked nature (53 MHz micro-bunching) of the KTeV neutral hadron beam, and use the non-prompt component of activity in a large plastic scintillator hodoscope as a measure of slow neutron fluence. The details of this analysis can be found in an internal CKM memo (CKM 50 at $http://www.fnal.gov/projects/ckm/documentation/public/CKM\_50.ps.gz$). The summary of that memo is included here:

"These estimates bound the VVS slow neutron deadtime to less than 10% from the kaon beam dump, and less than 25% from the upstream π^+ beam plug. These bounds are quite conservative, and the deadtime associated with low energy neutron fluence will likely be far less for the following reasons:

- The average energy of the KTeV hadron beam is about $\times 5$ that of CKM. Hence the neutron fluence/hadron in the CKM beam will be less.
- The visible energy threshold on the KTeV scintillator trigger hodoscope used in these estimates is 0.2 MeV, which is below most energy deposits of low energy neutron induced reactions. Consequently the KTeV trigger hodoscope efficiently samples the local neutron fluence. In contrast the lowest visible energy considered for the CKM VVS is 1 MeV, which corresponds to incident photon energies greater than 3 MeV on average. The $n + p \rightarrow d + \gamma(2.2MeV)$ reaction will usually deposit visible energy less than 1 MeV.
- The amount and geometry of the shielding between the CKM K^+ beam dump and the VVS is similar to the material between the KTeV neutral beam dump and the KTeV trigger hodoscope. The extrapolated neutron fluence limit from the upstream beam plug however ignores the large amount of integrated shielding between this upstream CKM beam element and the VVS. Hence the neutron fluence from the beam plug will likely be far below the upper limit determined from downstream detector elements of KTeV.

These estimates and simple arguments suggest that the VVS singles rate will not be swamped by low energy neutrons. These estimates do however underscore the importance of shielding of upstream beam elements. Experience at BNL and other low energy kaon beam facilities has shown that low energy neutron fluence can be significantly reduced with careful dump design and the use of neutron absorbers. Our next round of investigations should include simulation codes designed specifically for low energy hadron and neutron transport such as MARS and PICA."

As discussed in the CKM_50 summary above, the 1 MeV visible energy threshold in the VVS is above the average energy deposit of the $n + p \rightarrow d + \gamma(2.2MeV)$ reaction. If necessary the visible energy threshold can be raised from the nominal 1 MeV visible energy threshold with only a modest increase in the $K^+ \rightarrow \pi^+\nu\overline{\nu}$ background. The increase in background as a function of threshold is listed below in table 4. Raising the visible energy threshold to 2 MeV will effectively turn off the influence of the $n + p \rightarrow d + \gamma$ reaction, while allowing the $K^+ \rightarrow \pi^+\pi^0$ background to increase by only 20%. Further raising the visible energy threshold to 5 MeV ($\sim$ 15 MeV γ) will turn off the essentially all neutron induced nuclear reactions while increasing while raising the $K^+ \rightarrow \pi^+\pi^0$ background by just a factor of $\times 2$.

Given the tolerable slow neutron fluence inferred from KTeV data and the margin in VVS visible energy threshold, we expect that the ambient slow (< 5MeV) neutron fluence will not seriously degrade the live-time of the CKM Vacuum Veto System.

$K^+ \rightarrow \pi^+\pi^0$ Background .vs. VVS Threshold	
VVS Visible Energy Threshold	Relative $K^+ \rightarrow \pi^+\pi^0$ Background Level.
1 MeV	$\times 1.0$
2 MeV	$\times 1.2$
5 MeV	$\times 2.1$
10 MeV	$\times 3.9$
20 MeV	$\times 7.9$

Table 4: Relative Dependence of $K^+ \rightarrow \pi^+\pi^0$ background of VVS visible energy threshold.

3.3 VVS singles rates as a function of threshold

Q3. *What are the singles rates as a function of threshold expected in the photon veto systems?*

Tables 5 and 6 below contain the singles rates as a function of visible energy threshold in the VVS and FVS respectively for the Kaon component of the beam from the CKM GEANT beam and detector simulations. These data include all kaon decays, both upstream and in the detector and all kaon interactions. We have also simulated the contributions to these rates from the pion and proton components and the beam. These are negligible compared to those shown in the tables. The fast and thermal neutron rates discussed in section 3.2 above are not included here.

Visible Energy Threshold	Hit OR Rates [MHz]	Mean number of hits	Max Rates per per tube [KHz]
1MeV	7.24	38.29	302
3 MeV	7.04	32.73	239
6 MeV	6.86	28.14	185
10 MeV	6.72	25.46	164
20 MeV	6.54	23.05	130
30 MeV	6.22	9.21	59
60 MeV	3.69	3.94	22
100 MeV	2.69	3.56	18
200 MeV	1.96	3.00	13
300 MeV	1.54	2.59	10

Table 5: VVS K alone from a 33MHz beam generated by CKM Geant-Beam

Visible Energy Threshold	Hit OR Rates [MHz]	Mean number of hits	Max Rates per per tube [KHz]
1MeV	10.85	28.11	1400
3 MeV	10.47	21.94	1154
6 MeV	10.19	16.91	909
10 MeV	10.07	11.46	727
20 MeV	9.97	7.65	530
30 MeV	9.90	6.42	433
60 MeV	9.48	4.36	312
100 MeV	6.70	3.78	221
200 MeV	3.86	3.16	127
300 MeV	3.50	2.63	94

Table 6: FVS - K alone from a 33MHz beam generated by CKM Geant-Beam